Spatiotemporal forward solution of the EEG and MEG using network modelling

Viktor K. Jirsa[1], Kelly J. Jantzen[1], Armin Fuchs[1] and J.A.Scott Kelso[1]

Center for Complex Systems and Brain Sciences, Florida Atlantic University
Boca Raton, Florida 33431, USA
jirsa@walt.ccs.fau.edu

Abstract. Dynamical systems have proven to be well-suited to describe human coordination behavior such as the synchronization with auditory stimuli. Simultaneous measurements of the spatiotemporal dynamics of electroencephalographic (EEG) and magnetoencephalographic (MEG) data reveals that the dynamics of the brain signals is highly ordered and also accessible by dynamical systems theory. However, models of EEG and MEG dynamics have typically been formulated only in terms of phenomenological modelling such as fixed current dipoles or spatial current distributions. In the present paper we wish to connect the experimentally observable EEG and MEG dynamics with the underlying physiologically plausible neural dynamics. To do so, we develop a methodological framework, which defines the spatiotemporal dynamics of neural ensembles, the neural field, on a sphere in three dimensions. Using magnetic resonance imaging (MRI) we map the neural field dynamics from the sphere onto the folded cortical surface of a hemisphere. The neural field represents the current flow perpendicular to the cortex and thus allows for the calculation of the electric potentials on the surface of the skull and the magnetic fields outside the skull to be measured by EEG and MEG, respectively. For demonstration of the dynamics, we present the propagation of activation at a single cortical site resulting from a transient input. Non-trivial mappings between the multiple levels of observation are obtained which would not be predicted by inverse solution techniques. Considering recent results mapping large-scale brain dynamics (EEG, MEG) onto behavioral motor patterns, this paper provides a discussion of the causal chain starting from local neural ensemble dynamics through encephalographic data to behavior.

1 Introduction

Non-invasive techniques such as functional magnetic resonance imaging (fMRI), electroencephalography (EEG) and magnetoencephalography (MEG) provide entry points to human brain dynamics for clinical purposes, as well as the study of human behavior and cognition. Each of these imaging technologies provides spatiotemporal information about the on-going neural activity in the cortex. Analysis techniques of experimental spatiotemporal data typically involve the identification of foci of activity such as single or multiple dipole localization

(see [51,60] for an overview) in a three-dimensional volume. Other techniques emphasize the pattern approach which aims at the identification of distributed sources [51] or activity patterns, of which the latter are defined only on the two-dimensional surface spanned by the EEG and MEG detectors. These remain somewhat invariant during the time course and typically minimize a postulated norm such as the Gaussian variance (Principal Component Analysis or PCA) [15, 38,44] or non-Gaussian statistical independence (Independent Component Analysis or ICA) [48]. The latter may also be derived from a Bayesian framework[42]. Signal Source Projection or SSP provides a decomposition into patterns of activity which are physiologically or anatomically meaningful, by these means, however, restricting the possible solution space to the experimenters expectations. More ambitious techniques wish not only to decompose the spatiotemporal dynamics into meaningful patterns, but also identify equations which govern the dynamics of these patterns [6, 7, 30, 45, 46, 59]. Unfortunately, the successful application of these techniques has been typically limited to special cases in which the majority of the observed dynamics has already been well understood [30]. Spatiotemporal activity propagation of electro- and magnetoencephalographic signals has been represented by discretely coupled oscillator models (see chapter on source modeling in [60]) representing dipole sources. Spatially and temporally continuous models, so-called neural fields, were formulated by Wilson-Cowan [62, 63], Nunez [52] and Amari [2] in the 70s. With improving imaging techniques and the development of MEG these types of models experienced a renaissance [13,31,47,55,64]. These models are typically based on coupled neural ensembles in a spatially continuous representation using integral equations involving a time delay via propagation. Jirsa & Haken [31] generalized and unified the earlier models by Wilson-Cowan [62,63] and Nunez [52] and demonstrated that they describe the same system. The modeling on these different levels of organization has been phenomenological, i.e. only partially taking into account the specific neurobiological nature of the measured signal and its underlying mechanism of generation. Each level of description has been tackled separately, never in unison with other fields of research, and typically applying strong simplifications. For example, Steyn-Ross et al. [58] explain a hysteresis phenomenon called 'biphasic response' in the clinical human EEG during anesthesia. Their underlying neural model is based upon Liley's work [47] using a spatially uniform activity distribution in one dimension with a connectivity distribution which falls off exponentially, independent of the cortical location. Similarly, Jirsa et al. [33] also applied a one-dimensional model allowing, however, for varying spatial structure in activity distributions. Here, by applying neural field equations to a bimanual coordination situation, they predicted the spatiotemporal dynamics observed in the MEG and confirmed these experimentally. A set of equations, governing human bimanual coordination [19], was derived from these neural field equations. This connection between spatiotemporal brain dynamics and behavioral dynamics has become possible through the notion of functional units [31, 33,16] that serve as interfaces between neural and behavioral signals. Despite these successes, the simplifications made in these approaches do not take into

consideration a more detailed physiological and anatomical interpretation of the identified mechanisms, e.g. how an active area may be identified when a spatially uniform activity distribution is assumed [58], resulting in an effectively zero-dimensional point-like model and brain.

In the present paper we develop a framework which overcomes these simplifications and allows a quantitative comparison between experimental data and theoretical modeling. The neural model used here is based on Jirsa & Haken [31] which allows the connection to the behavioral dynamics through the concept of a functional input or output unit [16]. We form a synthesis of methodologies in order to systematically relate scales of organization from neural ensembles through EEG and MEG to behavioral dynamics (for strategic aspects of our approach, see the trilogy [40]). The conceptual steps are the following: We define a spatiotemporal neural field dynamics on a spherical geometry. This dynamics is mapped onto the folded cortical surface, thereby minimizing the spatial distorsions. Importantly, it is the propagation of neural activity that generates the forward solutions of EEG and MEG. For the simplest cortical architecture, we choose the experimental condition of an induced stimulus on the cortical surface and map the neural field dynamics on the different levels of organization: 1. cortex on a sphere; 2. unfolded cortex; 3. folded cortex; and 4. folded cortex in the skull generating EEG and MEG.

Our paper is organized as follows: First, we review the dynamics of coordination behavior and its neural correlates. Second, we discuss the foundation of neural field dynamics and develop a systematic treatment of functional units. Third, we elaborate the methodologies involved in traversing scales of organization from the level of neural ensemble to EEG and MEG, and discuss the example of neural field dynamics after an induced stimulus. Finally, we provide a discussion and an outlook to future work.

2 Brain and Behavior correlates in motor coordination

Periodic movements such as rhythmic finger tapping have developed to a paradigm in human coordination dynamics. Nonlinear dynamics provides the mathematical tools necessary to study such periodic processes by interpreting them as limit cycles. The motion of a single finger, decoupled from any other effects, has been modelled as a Van der Pol-Rayleigh oscillator [19] since it shows similar dynamical properties as the experimental biological system, such as transient behavior or amplitude dependence on movement frequency. Once the finger motion is coupled to other signals, such as an external periodic signal, then the relative phase $\phi = \phi_1 - \phi_2$ between the finger motion with its phase ϕ_1 and the additional signal with ϕ_2 becomes the meaningful descriptor of coordination. Following Kuramoto's work [43], this situation may be beautifully generalized to arbitrarily many oscillators as long as their limit cycle properties are preserved. However, not every relative phase ϕ is possible anymore. The coupling establishes a *symmetry breaking* by constraining the number of existing phase states. Moreover, not every existing relative phase is actually stable, but may

serve as an unstable state separating two stable states. When control parameters such as movement frequency are manipulated, certain coordination states may become unstable and the system exhibits a transition from one state to another. These systems become low-dimensional in the vicinity of such phase transitions as a consequence of a time-scale separation, mathematically known as the center manifold theorem (see e.g. [23]) or the enslaving principle [18, 20]. The system's slower components, which are typically only a few, determine the macroscopic dynamics because the faster components have already relaxed quickly to their stationary states. The latter, however, are determined by the slow variables. Hence it is sufficient to understand the low-dimensional dynamics of the slow components only. For concreteness, in the example of unimanual coordination, the relative phase ϕ between the two oscillators is the slow variable, in fact this is true for most coordination dynamics [39]. However, on a more critical note, coordination dynamics has mainly focussed on rhythmic movements only, and hence limit cycles, together with Kuramoto's theorem [43] apply. Since coordination dynamics has a wider scope than rhythmic movements, the reader might want to keep this constraint in mind. Using spatiotemporal symmetry arguments [19] the dynamics of the relative phase ϕ between two oscillators may be expressed as

$$\dot{\phi} = -\frac{\partial V}{\partial \phi} = -a \sin \phi - 2b \sin 2\phi \tag{1}$$

where a, b are constant parameters dependent on the movement frequency. Since ϕ is one-dimensional, it may always be expressed as a gradient dynamics with a potential $V(\phi)$. The dynamics of V is illustrated in figure 1: The two potential minima correspond to the stable movement patterns in-phase, $\phi = 0$, and anti-phase, $\phi = \pi$. The latter becomes unstable when the movement frequency increases which correponds to a decrease of the ratio b/a.

What are the neuronal correlates of behavioral phenomena? What are the neuronal correlates of behavioral laws such the one expressed in equ. (1)? The nature of the answer will again depend on the chosen level of description. We identify individual functionally relevant elements of neural dynamics which will then be placed in a coordination situation, i.e. they will be coupled. The experimentally accessible observables are provided by non-invasive techniques such as electroencephalography (EEG), magnetoencephalography (MEG) and structural and functional magnetic resonance imaging (MRI, fMRI). The first two techniques, EEG and MEG, are direct measures of activation of neuronal populations. EEG measures the electric potential on the skull surface, MEG measures (typically) the gradient of the radial component of the magnetic field just above the skull surface. Both signals are generated by the simultaneous neuroelectric activity of hundred thousands of neurons located in the neocortex and can be resolved spatially on the order of cm and temporally on the order of msec. Structural MRI provides the three-dimensional coordinates of neuronal tissue on the scale of mm. fMRI measures metabolic activity, hence providing an indirect measure of neuronal activation on the spatial scale of mm and temporal scale of sec. Thus EEG and MEG provide measures of neuronal correlates on the same time scale as human behavior, but do not provide direct measures of source locations;

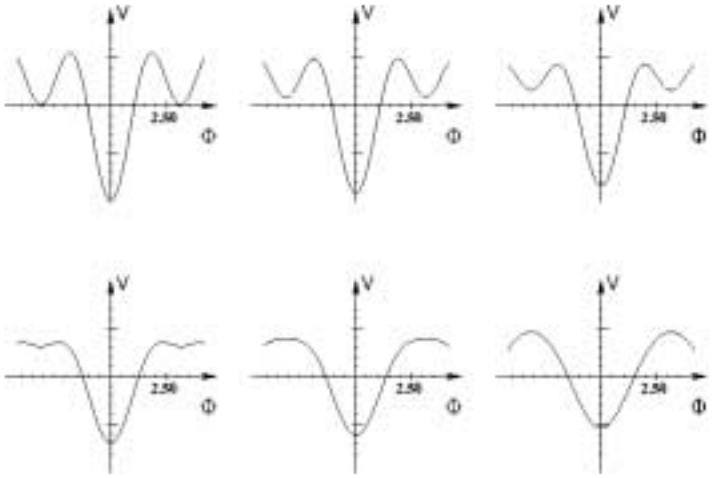

Fig. 1. The $V(\phi) = -a\cos\phi - b\cos 2\phi$ is plotted in dependence of the ratio b/a, decreasing from 1 to 0, from left to right starting with the top left graph. The minima represent stable stationary states of the gradient dynamics $\frac{\partial\phi}{\partial t} = -\frac{\partial V}{\partial\phi}$.

on the other hand, fMRI provides accurate measurement of neural sources, but is an indirect measure and too slow to capture human behavioral dynamics.
Following the strategy on the behavioral level, we define an isolated spatiotemporal event, a rhythmic finger movement, and identify its neuronal correlate. Particularly, sensori and motor events are well represented in EEG and MEG dynamics, thus are well-suited for investigation of its dynamics. Let us assign the variable $r(t)$ to the coordinate of the finger motion as a function of time t. We wish to express the finger's dynamics as a function of neuronal activity $\Psi(x,t)$ defined in physical space x and time t. Which neuronal activity? What physical space? Initially, let us identify Ψ with the measured variable, that is for EEG the electric potential, and identify the physical space to be defined by the EEG electrodes. Obviously, there is a relation between the spatiotemporal pattern in the EEG and the underlying neuronal generators which is known as the inverse problem. We, however, seek to identify the dynamics of the patterns in the EEG and MEG, not to solve the inverse problem in the first place. Recent MEG experiments ([41]) have shown that the finger velocity is actually strongly correlated with the MEG patterns. This correlation will be expressed mathematically (see the section 3.1) and used in the following to map the brain and behavior correlates onto each other. In particular during rhythmic movement

tasks a linear relationship between the neuronal activation $\Psi(x,t)$ and the finger movement $r(t)$ exists [15, 41, 39, 21]. Such a behavior may be safely assumed to be a consequence of the averaging of higher order harmonics of the dominating frequency. Mathematically the averaging corresponds to the rotating wave approximation [18, 20]. For concreteness, let us again consider the unimanual finger motion: Previously in the behavior, the finger motion, $r(t)$, has been coordinated with the metronome signal $s(t)$ resulting in an interaction and creating the two stationary movement patterns in-phase and anti-phase ; these movement patterns correlate strongly with spatiotemporal neuronal patterns as measured with a 37-dimensional SQuID (superconducting quantum interference device) array [38] and illustrated in figure 2.

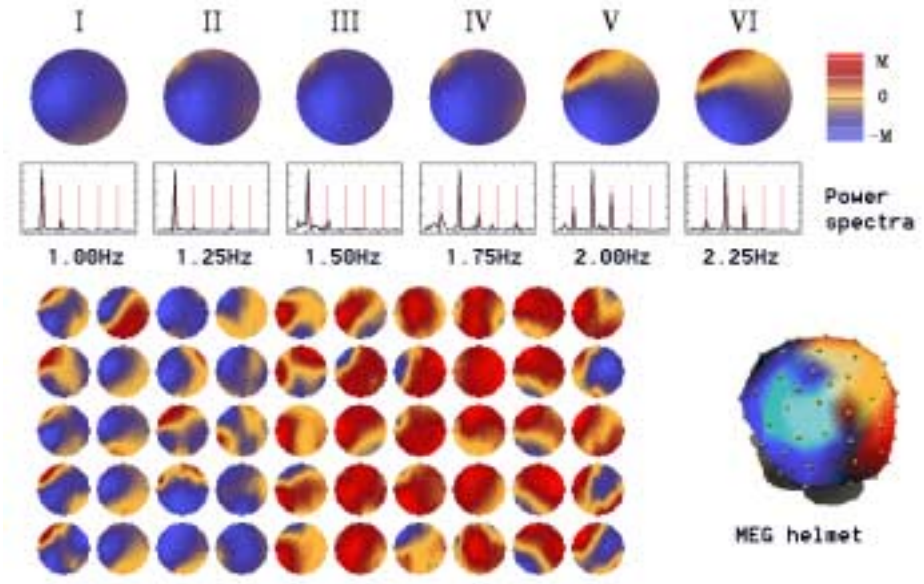

Fig. 2. Unimanual finger movement and its MEG. A 37-dimensional SQuID array was placed over the left hemisphere as illustrated in the bottom right graph. For six plateaus, corresponding to stimulation frequencies 1Hz through 2.25Hz, the dominant spatial structure is plotted in the top row, together with its power spectrum. In the latter, the vertical red lines denote the stimulus frequency and its higher harmonics. The phase transition in behavior occurs on plateau IV, coincident with a change in the spatial patterns and the power spectra. An example space-time series of five cycles on plateau II is plotted in the bottom left.

The MEG detectors were located centrally over the primary motor and auditory areas of the left hemisphere. The subject was instructed to perform a

right-handed finger movement in anti-phase with an auditory metronome starting at frequencies of 1Hz and increasing in steps of 0.25Hz. Intervals of constant stimulus frequency are referred to as plateaus. Analyses [15] showed that the first two spatial principal components carry about 80% of the variance of the entire MEG signal. Later analyses [30] showed that these patterns are obtained as projections, $\Psi_i(t) = \int_\Gamma \beta_i(x)\Psi(x,t)dx$, of the neuronal activity onto the individual spatial templates $\beta_i(x)$, $i = 1, 2$. In contrast to PCA, these templates may be linearly dependent. As shown in the first row of figure 2, the strongest pattern of each plateau carries about 60% of the variance of the MEG signal. Before the transition, on plateaus I-III, the first pattern dominates. A transition occurrs on plateau IV and a new pattern emerges on plateaus V and VI when the subject actually performs an in-phase motion. This transition from one pattern, Ψ_1, to another pattern, Ψ_2, is accompanied by a transition in the frequency domain: On plateaus I through III, the observed MEG pattern oscillates mainly with the movement frequency, and on plateaus V and VI mainly with twice the movement frequency. As an example of the spatiotemporal sequence for constant stimulus frequency, figure 2 shows 5 cycles of the measured MEG patterns at different time instances. This sequence is taken from plateau II and clearly exhibits the dominance of the pattern Ψ_1 extracted in the earlier analysis, figure 2 (top left). Subsequent phenomenological modelling of the MEG pattern dynamics revealed that the phenomena may be understood as the nonlinear interaction of the two patterns Ψ_1 and Ψ_2 under the impact of an external periodic driver, in this case the auditory metronome $s(t)$ [29, 30]. If one accepts this hypothesis, then it actually follows that the coupling between the MEG patterns Ψ_1, Ψ_2 and the metronome $s(t)$ has to be multiplicative, a so-called parametric driving [29]. Referring back to our earlier discussion, MEG patterns correlate strongly to the corresponding movement patterns. Hence, if we can identify the mapping between the MEG patterns and the movement patterns, then we can also derive the functional form of the coupling between finger movement $r(t)$ and stimulus signal $s(t)$. For unimanual coordination the parametric driving proves to be a strong candidate for the $r(t)$-$s(t)$-coupling and signatures of parametric driving have been found in two recent behavior experiments [3, 12, 34]. The dynamic mechanism on both levels of description, the neuronal and behavioral levels, is of the same generic type, a Pitchfork bifurcation.

3 Methods

3.1 Neural field dynamics

We choose a macroscopic level of description, the neural ensemble, which is appropriate for the EEG and MEG. The structure of our model is generic and found in most models describing neuronal activity: a firing rate of a neuronal ensemble at a location A is transmitted to a neuronal ensemble at a distant location B. Most models differ in variations of connectivity and inclusion of physiological detail. In the present neuronal field model, a time delay via transmission is considered due to the large spatiotemporal scales of interest. The following three

specific properties distinguish the present neuronal field model from most other approaches: 1) Conversion operations [31] define mathematical relations between firing rates and local field potentials. Research by Freeman [14] and others [1], [57] showed in a variety of cortical areas that the neuronal firing rate and the local field potential are related in a well-defined way (the so-called conversion operations [14]): Dendritic currents generated by active synapses cause extracellular local field potentials that can be measured by EEG [14], and intracellular currents measurable by MEG [61]. The conversion from local field potential to firing rate within a neuronal ensemble is sigmoidal. The inverse conversion, from firing rate to local field potential, is also sigmoidal, but constrained to a linear small-signal range. 2) To capture the large spatial and temporal scales in EEG and MEG, the connectivity includes both, the short range intracortical fibers (excitatory and inhibitory), which typically have a length of 0.1 cm, and the corticocortical (only excitatory) fibers with lengths ranging from about 1 cm to 20 cm [52]. Propagation along these long range fibers may cause time delays up to 200 msec. The distribution of the intracortical fibers, and thus the local connectivity, is homogeneous [5], whereas the distribution of the corticocortical fibers is not (estimates are that forty percent of all possible corticortical connections are realized for the visual areas in the primate cerebral cortex [11]). For these reasons an inhomogeneous interareal connectivity has to be allowed resulting in a translationally variant connectivity function $f(x,X) \neq f(x-X)$. External input $p_j(x,t)$ is realized such that afferent fibers make synaptic connections. Then the neural field dynamics may be written as

$$\psi(x,t) = \int_\Gamma dX\, f(x,X) \cdot S[\psi(X, t - \frac{\mid x-X \mid}{v}) + \sum_j p_j(X, t - \frac{\mid x-X \mid}{v})] \ , \quad (2)$$

where Γ represents the closed two-dimensional surface. The neural field equation (2) can be transformed into a partial differential equation for a homogeneous connectivity function $f(x,X) = f(\mid x-X \mid)$ such as $e^{-|x-X|/\sigma}$. Then the nonlinear partial differential equation reads in one dimension

$$\ddot{\psi} + (\omega_0^2 - v^2 \triangle)\ \psi + 2\omega_0 \dot{\psi} = (\omega_0^2 + \omega_0 \frac{\partial}{\partial t}) \cdot S[\psi(x,t) + p(x,t)] \quad (3)$$

where $\omega_0 = v/\sigma$. In case of a general connectivity function, an integral representation has to be maintained. 3) Finally, functional units relate neuronal events to external events and are discussed in detail in the following section.

3.2 Functional units

Functional units represent interfaces between the neocortex and non-cortical (input and output)signals and include subcortical structures such as the projections of the cerebellum on the cortex or specific functional areas such as the motor cortex. Until now the spatial localizations of functional units have been identified with the spatial patterns which are observed in the EEG/MEG and generated by time dependent input signals (e.g. see [41]). This is due to the fact

that the description and the modelling of EEG/MEG dyamics has been almost exclusively in terms of patterns rather than cortical sources. In the case of a finger movement, this spatial structure corresponds to a dipolar pattern in the EEG/MEG located over the contralateral motor cortex. Anatomically these areas are obviously defined via their afferent and efferent fibers connecting to the cortical sheet. As such we will treat these in the spirit of this paper, a realistic treatment of brain signals, architecture and its resulting EEG/MEG. We define the j-th functional input unit $p_j(x,t)$ (see [16] for a detailed treatment) by its location $\beta_j(x)$ on the folded cortical sheet and a time dependent peripheral signal $r_j(t)$ (such as a finger movement)

$$p_j(x,t) = \beta_j(x) \int_{t_0}^{t} f(t-\tau) r_j(\tau) d\tau \tag{4}$$

where t_0 is the initial time point and $f(t-\tau)$ a yet unknown convolution function. As mentioned earlier, for rhythmic movements the peripheral signal and the neural activity of the functional units seems to be linearly related (see [16] for details), hence the linear term r_j in (4). Along the same lines a functional output unit may be constructed,

$$r_j(t) = \int_\Gamma dx\ \beta_j(x) \int d\tau\ g(t-\tau)\psi(x,\tau)\ , \tag{5}$$

where $\beta_j(x)$ defines the spatial location of the output unit in the cortical sheet and $g(t-\tau)$ an yet unknown convolution function. This read-out procedure may be viewed as a rule for how neural currents drive the finger movement represented as an oscillator.

On the large spatiotemporal scale of EEG/MEG the input and output localizations can not be distinguished, hence we approximate them to be equal, i.e.

$$\beta_j^i(x) \approx \beta_j^o(x) = \beta(x) \tag{6}$$

and drop the index j since we will be concerned with one spatial localization only. We define the integral operators

$$\hat{L}_0 = \int_{t_0}^{t} g(t-\tau)d\tau\ , \qquad \hat{L}_1 = \int_{t_0}^{t} f(t-\tau)d\tau\ , \qquad \hat{L}_s = \int_\Gamma \beta(x)dx \tag{7}$$

acting on functions in the space L_2 where $\hat{L}_s$ commutes with $\hat{L}_0$, $\hat{L}_1$ and $\hat{L}_s\beta(x) = N \in \mathcal{R}$ where the latter is a projection operator under proper normalization.

We rewrite (4),(5) as

$$r(t) = \hat{L}_s\hat{L}_0\psi(x,t) = \hat{L}_0\hat{L}_s\psi(x,t) \tag{8}$$

$$\hat{L}_s p(x,t) = N\hat{L}_1 r(t) = \hat{L}_1\hat{L}_0\hat{L}_s\psi(x,t) \tag{9}$$

where we applied $\hat{L}_s$ in the latter. We expand $r(t)$ in (9) around the time point t and obtain

$$\ldots + c_2\ddot{r}(t) + c_1\dot{r}(t) + c_0 r(t) = \frac{1}{N}\hat{L}_1\hat{L}_0\hat{L}_s\psi(x,t) \tag{10}$$

where

$$c_n = \int_{t_0}^{t} f(t-\tau)\frac{(\tau-t)^n}{n!}d\tau \tag{11}$$

Kelso et al. [41] found experimentally that the brain patterns $\mathbf{v}^1 = (\cdots v_k^1 \cdots)$ and $\mathbf{v}^2 = (\cdots v_k^2 \cdots)$ can be decomposed as

$$\psi_k(t) = r(t)\ v_k^1 + \dot{r}(t)\ v_k^2 \tag{12}$$

where $\psi_k(t)$ is the MEG amplitude at the k-th sensor. It turns out that the velocity is the dominant contribution, i.e. $\mid \mathbf{v}^1 \mid \ll \mid \mathbf{v}^2 \mid$. Hence we make the identification

$$\mathbf{v}^2 \longrightarrow \beta(x) \qquad \text{with} \qquad \mathbf{v}^2\mathbf{v}^2 = N \longrightarrow \hat{L}_s\beta(x) = N \tag{13}$$

in the continuous limit. We multiply (12) by $\mathbf{v}^2$, i.e. apply $\hat{L}_s$, and obtain

$$\dot{r}(t) + \frac{\mathbf{v}^1\mathbf{v}^2}{N}\ r(t) = \frac{1}{N}\hat{L}_s\psi(x,t) \tag{14}$$

in the continuous representation. Comparing the experimental result (14) with the theoretical result (10) we find

$$c_0 = \frac{\mathbf{v}^1\mathbf{v}^2}{\mathbf{v}^2\mathbf{v}^2} \qquad c_1 = 1 \qquad c_2 = c_3 = ... = 0 \tag{15}$$

and

$$\hat{L}_1\hat{L}_0 = \hat{I} \tag{16}$$

where $\hat{I}$ is the identity operator. There is one additional freedom, namely the scaling of either $r(t)$ or $\psi(x,t)$ which introduces the scaling parameter ϵ. With (15), (16) we rewrite (10) as

$$\dot{r}(t) + c_0\ r(t) = \epsilon \int_\Gamma \beta(x)\ \psi(x,t)\ dx \tag{17}$$

where the lhs represents the intrinsic dynamics of the finger motion and the rhs the excitation by the brain signals, thus we can interprete the finger movement as an overdamped oscillator driven by the brain signals which are projected onto the functional output unit. The solution of (17) reads

$$r(t) = \epsilon \int_\Gamma \beta(x) \int_{t_0}^{t} g(t-\tau)\ \psi(x,\tau)\ d\tau\ dx \tag{18}$$

with the transfer function

$$g(t-\tau) = e^{-c_0(t-\tau)} \tag{19}$$

and the initial time point far in the past, i.e. $t_0 \approx -\infty$. Using (10),(15) the integral operator $\hat{L}_1$ can be written as

$$\hat{L}_1 = \int_{t_0}^{t} f(t-\tau)d\tau = \frac{\partial}{\partial t} + c_0 \tag{20}$$

and its transfer function

$$f(t-\tau) = c_0\delta(t-\tau) + \frac{\partial}{\partial t}\delta(t-\tau) \tag{21}$$

where $\delta(t-\tau)$ is a δ-function.

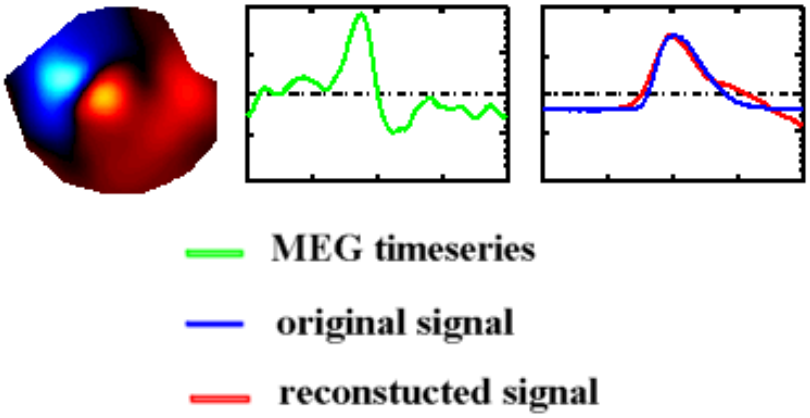

Fig. 3. Functional unit of a right-handed motor movement. The spatial MEG pattern, that is $\beta(x)$, is shown on the left which represents the dominant spatial structure present in the MEG signals obtained from a 64-sensor full-head detector. Here the unfolded brain map is shown, that is nose on the top, left ear is left, right ear is right. In the middle, the time series obtained from the projection onto the functional unit, $\int_\Gamma dx\beta(x)\psi(x,t)$, is shown. On the right, the time series showing the experimental finger movement $r(t)$ is plotted in blue, and the reconstruction using the functional unit (see equ. (18)) is plotted in red. All the time series range from -500msec to 500msec with maximum flexion at $t = 0$.

Our main results are the equations (13),(15),(18) and (19). Here (18) defines an explicit relation between on-going brain activity $\psi(x,t)$ measured by EEG/MEG and rhythmic finger movement $r(t)$. There is only one free scaling parameter, ϵ, all other terms are experimentally accessible and well-defined. Figure 3 shows the reconstruction of the movement profile from neural activity according to (18). Note the reconstructed movement profile fits the experimentally observed movement particularly well in the active phase represented by its positive flank. The discrepancies mainly occur after peak displacement and are probably due to the sensory feedback which is not accounted for by (18).

3.3 Neural field dynamics on a sphere

The neural field equation (2) is defined in two dimensions with spherical boundary conditions. For a homogeneous, exponentially decaying connectivity function the corresponding partial differential equation may be determined:

$$(\frac{\partial^2}{\partial t^2} + 2\omega\frac{\partial}{\partial t} + \omega_0^2 - v^2\triangle)^{3/2}\,\psi = (\omega_0^3 + \omega_0^2\frac{\partial}{\partial t}) \cdot S[\psi(x,t) + p(x,t)] \qquad (22)$$

The details of the differential operators on the lhs of (22) depend on the spatial decay of the connectivity. However, these details are not significant for large scale pattern formation as shown by Haken [22]. Each cortical hemisphere is represented in a spherical geometry and its dynamics is defined by (2), or (22), respectively. The two spheres interact by two means: through calossal pathways connecting the two spheres and through afferent fibers (crossing and non-crossing) from the periphery. Subcortical regions such as the brainstem are not included. Should heterogeneous fiber pathways be included also, then the integral representation given by (2) is used and two types of pathways distinguished: 1. The calossal fiber system from one sphere to another is treated in a manner equivalent to peripheral afferents. 2. Other heterogeneous pathways are included in the connectivity function $f(x, X)$. Note that heterogeneous pathways contribute strongly to the dynamics on all scales of organization; even local changes of connectivity have recently been shown to result in a major reorganization of brain activity [35, 36].

3.4 Unfolding of the cortical sheet and its spherical representation

In order to equate the distribution of neural fields with actual cortical structure a mapping between the spherical surface and the cortical surface is required. Several steps are undertaken to complete this mapping. All of the described procedures were performed using the Freesurfer software package developed by Dale and colleagues [9, 10]. The first step is the segmentation of the brain structure and the definition of the gray-white matter boundary within each hemisphere. This step allows for the description of the cortical surface by a mesh defined by a set of vertices and polygons. The second step involves the inflation of the cortical surface to produce a closed surface that has minimal folding but also minimizes any distortion in the relative location between cortical locations (see middle image of figure 4). This step eliminates the difficulty of visualizing cortical activity within sulci. The final step is to transform this shape onto a spherical representation while maintaining as much of the spatial relation as possible by preserving the metric properties of the surface while minimizing the local curvature. With this procedure, any point on the folded cortex can be addressed using any number of coordinate systems via its isometric location on the neural sphere. Both transformations, forward and backward, are well defined and their product yields the identity. Figure 4 gives an impression of this process by showing the three surfaces with the cortical surface color coded in red and blue according to curvature. A spherical coordinate grid is plotted in green with the line of zero

longitude in white. The resulting meshes are extremely dense typically involving on the order of 150,000 vertices for the representation of a single hemisphere. For the purpose of computational frugality we decimated this tessellation to a more manageable number of vertices and corresponding polygons, 4512 and 9022 respectively.

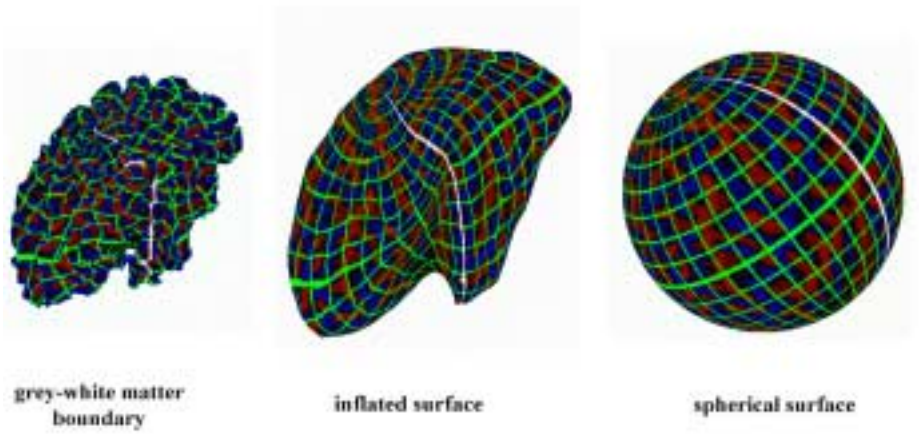

Fig. 4. Inflating the surface representing the gray-white matter boundary and mapping onto a sphere. From right to left the sequence shows how a spherical coordinate grid gets folded into the fissures.

3.5 Representation of neural fields on the folded cortex

In the previous section we described how each hemisphere was expanded and warped onto a sphere. As a result of this transformation, each sampled vertex on the folded cortical surface has a corresponding vertex located on the surface of a sphere. In addition to this one-to-one mapping between the vertices defining both the surface of the cortex and a sphere, the connectivity of the polygons (i.e. how the vertices are connected) remains constant across this transformation. The description of activity on the surface of the spherical hemisphere is automatically mapped onto the surface of the cortical representation. The task, therefore, simplifies to the mapping of the activity onto the surface of an irregularly sampled sphere. This is a simple matter, however, because the neural field is continuous across the sphere on which it is generated and therefore can be sampled at any arbitrary point. The mesh vertices of the cortical sphere are easily converted to spherical coordinates and the value at the corresponding location of the neural field sphere is assigned. However, caution has to be taken when the space-time

structure of the neural field dynamics on the sphere is compared to the one on the folded cortex. The non-conformal mapping of the Freesurfer software alters the distances between adjacent vertex points and hence the neural field dynamics. Fischl et al. [10] report an average local error of 20% between folded cortical and spherical coordinate system. In numerical simulations of neural fields which were homogeneously connected we did not find any obvious discrepancies between the dynamics in both systems which is probably a consequence of the integration process in (2) resulting in a averaging of the error. Research of detailed error calculations of the space-time structure is on-going.

For graphical presentation, the field distribution over the cortical surface can be represented as a set of color values scaled between the maximum and minimum field strength. Changes in this color representation over time then give a temporal depiction of how the field dynamics unfold on the actual cortical surface. However, in order to calculate the forward solution using these current densities we need the additional information about the direction of current flow at each vertex location and each point in time. The generation of local field potentials within the cortex is dominated by activity in ensembles of pyramidal cells, which are oriented perpendicular to the cortical surface. It is possible therefore to model the direction of instantaneous current flow in a small cortical region as a normal vector on the mesh surface. The orientation of the vector gives the direction of current flow and the length of the vector gives the current strength. For the purpose of mapping neural activations onto the representation of the cortical surface a vector oriented normal to the polygon surface was computed for each mesh vertex. These vectors were then normalized to a length of one and scaled by the amount of neural activation at each time point. Because the direction of current flow is given by the orientation of the cellular generators, orientation of these vectors does not change over time (see following section 3.6 for details). Instantaneous current flow is always represented by vectors oriented orthogonal to the cortical surface while the propagation of current flow across the cortical surface is modelled as changes in the absolute and relative strengths of these vectors over time.

3.6 Generating EEG and MEG from the neural field dynamics

At this stage we have a representation of the current distribution in three-dimensional space $x \in \mathcal{R}^3$ and its evolution over time t. To make a comparison with experimental data the forward solutions of the scalar electric potential $V(x)$ on the skull surface and of the magnetic field vector $\mathbf{B}(x)$ at the detector locations have to be calculated. Here it is useful to divide the current density vector $\mathbf{J}(x)$ produced by neural activity into two components. The volume or return current density, $\mathbf{J}^v(x) = \sigma(x)\mathbf{E}(x)$, is passive and results from the macroscopic electric fields $\mathbf{E}(x)$ acting on the charge carriers in the conducting medium with the macroscopic conductivity $\sigma(x)$. The primary current density is the site of the sources of brain activity and is approximately identical to the neural field $\psi(x,t)$, because, although the conversion of chemical gradients is due to diffusion, the primary currents are determined largely by the cellular-level details

of conductivity. In particular, cell membranes, being good electrical insulators, guide the flow of both intracellular and extracellular currents and thus result in a current flow perpendicular to the cortical surface due to the perpendicular alignment and elongated shape of pyramidal neurons. In the quasistatic approximation of the Maxwell equations, the electric field becomes $\mathbf{E} = -\nabla V$ where ∇ is the Nabla-operator $(\ldots \partial/\partial x \ldots)^T$. The current density $\mathbf{J}$ is

$$\mathbf{J}(x) = \psi(x,t)\mathbf{n}(x) + \sigma(x)\mathbf{E}(x) = \psi(x,t)\mathbf{n}(x) - \sigma(x)\nabla V(x) \tag{23}$$

where $\mathbf{n}(x)$ is the cortical surface normal vector at location x.

The forward problem of the EEG and MEG is the calculation of the electric potential $V(x)$ on the skull and the magnetic field $\mathbf{B}(x)$ outside the head from a given primary current distribution $\psi(x,t)\mathbf{n}(x)$. The sources of the electric and magnetic fields are both, primary and return currents. The situation is complicated even more by the fact that the present conductivities such as the brain tissue and the skull differ by the order of 100. Following the lines of Hämäläinen et al. [24,25] and using the Ampére-Laplace law, the forward MEG solution is obtained by the volume integral

$$\mathbf{B}(x) = \frac{\mu_0}{4\pi} \int (\psi(X,t)\mathbf{n}(X) + V(X)\nabla'\sigma(X)) \times \frac{X}{\mid X \mid^3} dv' \tag{24}$$

where dv' is the volume element, ∇' the Nabla-operator with respect to X and μ_0 the magnetic vacuum permeability. The forward EEG solution is given by the boundary problem

$$\nabla \cdot (\sigma(x)\nabla V(x)) = \nabla \cdot (\psi(x,t)\mathbf{n}(x)) \tag{25}$$

which is to be solved numerically for an arbitrary head shape, typically using boundary element techniques as presented in [24,25]. In particular, these authors showed that for the computation of neuromagnetic and neuroelectric fields arising from cortical sources, it is sufficient to replace the skull by a perfect insulator, and, therefore, to model the head as a bounded brain-shaped homogeneous conductor. Three surfaces S_1, S_2, S_3 have to be considered at the scalp-air, the skull-scalp, and the skull-brain interface, respectively, whereas the latter provides the major contribution to the return currents. The three-dimensional geometry of these surfaces may be obtained from MRI scans.

4 Results

To illustrate the simultaneously ongoing dynamics on the different levels of organization we choose a simple example of induced wave propagation along the cortical sheet. The connectivity is spatially homogeneous and has an exponential fall-off. Only one functional unit, the stimulus input, is defined just posterior to the central fissure, otherwise the neural sheet is completely homogeneous and isotropic. For visualization purposes, only one hemisphere is shown in the following.

At time $t = 0$ a stimulus signal $r(t)$ is sent to the cortical sheet through afferent fibers via synaptic connections defined by $\beta(x - x_0) = e^{-|x-x_0|}$. The time course $r(t)$ is an exponential increase until t=160ms, then followed by an exponential decrease (plotted on the bottom of figure 5). The stimulus excites the neural sheet at site A, $x = x_0$, and initiates wave propagation by means of a circular traveling wave front undergoing attenuation in space and in time. The time courses of the neural ensembles at site A and site B, which is more distant to the stimulus site, are shown. For several selected time points the spatiotemporal activity patterns on the sphere are plotted in the top row of figure 5. Here and in the following the color code represents -MAX to MAX as blue goes through black to yellow. In the rows below, the same neural activity patterns are represented on the unfolded cortex and on the folded cortex for the same time points after being mapped from the spherical representation following sections 3.4 and 3.5. Note that the circular travelling wave structure is preserved in both, the folded cortical and the spherical coordinate system implying that the error caused by the non-conformal coordinate transformation is not too significant, at least for the present case of purely homogeneous connectivity.

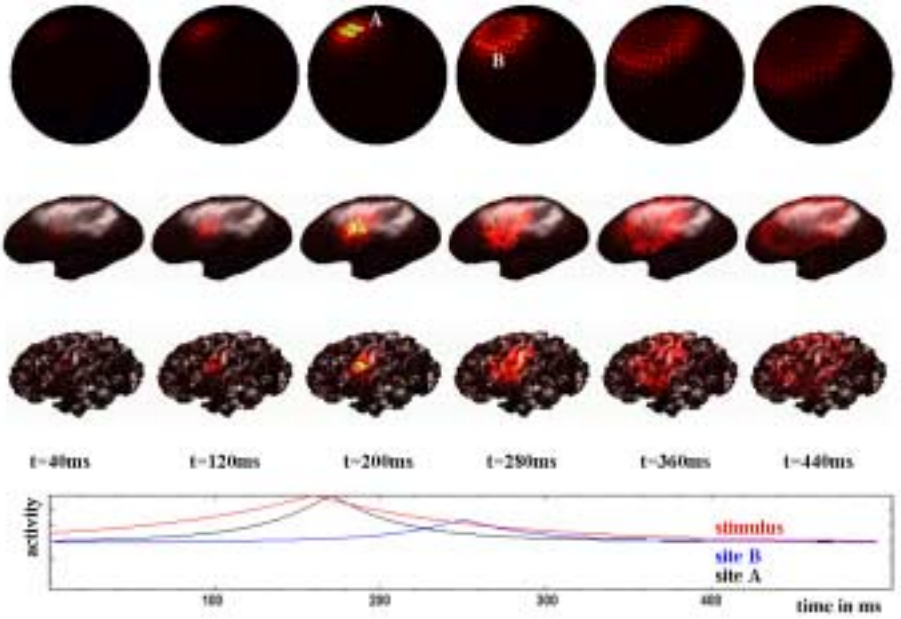

Fig. 5. The neural fields evoked by a transient stimuli distributed on the sphere (top row), inflated cortex (second row) and folded cortex (third row) for 6 separate time points. The bottom panel shows the time course of the stimulus (red line) and the activation pattern for two individual sites on the spherical surface.

For purposes of calculation of the forward EEG and MEG solutions, we use a single layer head model (skull-brain) as defined in 3.6 and a spherical head shape. The three-dimensional current distribution is defined on the folded cortical surface located within the skull as illustrated on the bottom in figure 6 (upper skull surface is not shown). The color coding on the cortical surface reflects the local curvature at the vertices with blue and red indicating convex and concave curvature, respectively. Note that the cerebellum is not part of these surfaces and has been removed. Adjacent is plotted the three cross sections of the voxel distributions showing the neural activity pattern color coded for t=200ms. The EEG and MEG detectors are placed directly on the spherical skull surface, infinitely close to each other. For the MEG we assume radial gradiometers measuring the radial component of the magnetic field $\mathbf{B}$. We calculate the forward solutions of the EEG and MEG measured by these detectors following (24),(25) and plot the resulting EEG (top row) and MEG (second row) patterns for the selected times. Note that the visualization is in the spherical system, the nose pointing to the left, basically resembling the perspective shown in the picture on the bottom left of figure 6. In both patterns, EEG and MEG, a dipolar structure emerges with a maximum activity at around 280ms for the EEG and two maxima for MEG at around 200ms and 360ms. From figure 5 it is clear that the neural current distribution is damped and flattens out as time evolves. However, the propagation of the neural wave front along the cortical surface is such that the neuromagnetic forward solution not only undergoes a spatial reorganization from 360ms to 440ms, but also a temporal organization which does not map trivially on the neural field activity.

Elaboration of this model will proceed not only at the neural level or even at the macroscopic EEG and MEG level, but also at the behavioral level. That is, the goal is not to simply reproduce observed spatiotemporal data sets by activating specific cortical regions, but to describe and explain behavioral phenomenona via the dynamics within and between interconnected cortical and subcortical areas. For instance, several properties of spatiotemporal cortical activity, as measured by EEG and MEG, have been shown to accompany behavioral transitions in coordinative states [17, 28, 38, 49]. We discussed one example, unimanual coordination, in section 3. At present the link between these specific neural events and the resulting behavioral dynamics is unknown in general, except for special cases such as rhythmic coordination [16]. This is despite the fact that much is known about the neural structures involved in producing coordinated movements and how they are connected to one another. Similar phenomena have been investigated using a one dimensional model of neural field dynamics [31, 30, 33] and it is expected that the application of the current model in its present and future forms will continue to provide insight into behavioral phenomena.

It should be emphasized that the model presented here is not a form of inverse solution that defines putative neural sources associated with a particular experimental design and set of data. The mapping of neural fields onto the folded cortex and the calculation of the forward solution are performed for the purpose of connecting cortical dynamics with neurophysiological and behavioral results.

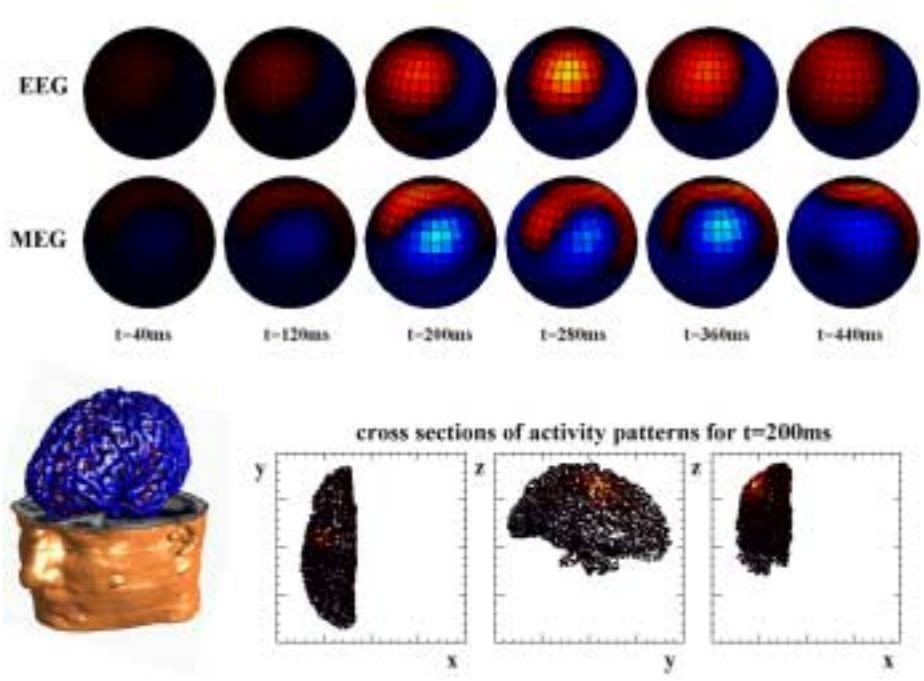

Fig. 6. The EEG (top row) and MEG (second row) forward solutions calculated at the same 6 time points as shown in figure 5. The activation patterns are plotted on a spherical head model used in the forward calculation (10 cm diameter). The spherical head model is oriented such that the nose is to the left of the page and the left side of the head is facing the reader. The location of the left cortical hemisphere used here is given within both the head of the subject (bottom left) and within the spherical model of the head (three views on the bottom right).

The data that result from the model are purely a function of the dynamics of the defined system, and are not constrained by observed data. It is possible therefore, to define a single dynamical model that can explain several different phenomena that may arise by changing input/output patterns. That is, the same model may generate qualitatively different data given different types of inputs or different output constraints. Such a system may also explain changes in perceptual phenomena despite the constancy of a stimulus (so-called bistable stimuli). This model then represents a powerful tool capable of representing the complexities that define human brain and behavior.

5 Final remarks and future directions

Here we present a conceptual and methodological framework for the development of a theoretical model of human brain function and behavior that operates

at multiple levels of description. Interconnected neural ensembles with homogeneous connection represent a neural level, while a network or systems level is defined by the interaction between heterogeneously connected cortical regions. An even broader level is defined by the computation of the spatiotemporal dynamics of EEG and MEG generated by the model and the connection of these data to behavioral dynamics. For concreteness: what is the neural substrate of the coupling between left and right finger within the bimanual coordination paradigm? Heterogeneous fiber tracts that connect the cortical, subcortical and spinal subsystems involved in coordination tasks still have to be implemented in our platform. These pathways couple the subsystems and thus add to their cross-talk and the resulting coordination dynamics. The heterogeneities introduce additional entries in the connectivity matrix of the neural field [36] carrying the information on distance and strength of coupling between areas. In the near future, developing technologies, such as diffusion tensor weighted imaging (DTI), promise to provide complete information of the white matter tracts in the connectivity matrix of individual subjects [4], [54]. Developmental studies have reported that mirror movements appear as normal phenomena in young children; such mirror movements occur as mirror reversals of an intended movement on the other side of the body and disappear after the first decade of life, coinciding with the completion of myelination within the corpus callosum [8],[65] and implying the involvement of callosal fibers in bimanual cross-talk. These fibers are known to transmit both inhibitory and excitatory influences [50] and are generally topographic, that is, they go to homologous points in the contralateral hemisphere. Also, the involvement of subcortical structures and additional cortical areas during coordination is known. For example, the cerebellum is activated ipsilaterally during unimanual finger movements, but sometimes bilaterally recruited during sequential unimanual movements [26]. Supplementary motor areas (SMA) also show increased activation (fMRI [27], positron emission tomography (PET) [56]) for bimanual than for unimanual activity.

This collection of neurophysiological and anatomical facts provides evidence on the coupling which mediates the information transfer during coordination, i.e. its neural basis established by matter such as callosal fibers, cerebellar contributions, etc. . On the other hand, from the dynamics' perspective we provided the descriptions and laws of coordination on selected levels of organization: the dynamics of the behavioral patterns and the dynamics of the corresponding neuronal patterns. A description in terms of neuronal activity patterns aids in developing the first contacts between generic pattern formation mechanisms and physiological quantities. The three-dimensional basis, developed throughout this article, finally sets the stage on which non-invasive brain imaging techniques, theory and modelling, as well as spatiotemporal data analysis merge together to address questions in behavioral neuroscience. We guided the reader through our approach conceptually and along the specific example of unimanual coordination. Its extensions to other domains of neuroscience, such as learning or impairments, are numerous and left to the reader.

Acknowledgements

This research was supported by NINDS Grant NS-39845 to AF, NIMH Grants MH-42900 and MH-01386 to JASK and the Human Frontier Sciences Program. We would like to thank James Duncan for helpful comments on the transformation from the spherical to the cortical system.

References

1. Albrecht, D.G., Hamilton, D.B.: Striate cortex of monkey and cat: contrast response function. J. Neurophys. **48** (1989) 217-237
2. Amari, S.: Dynamics of pattern formation in lateral-inhibition type neural fields. Biol. Cybern. **27** (1977) 77–87
3. Assisi, C.G., Jirsa, V.K., Kelso, J.A.S.: Dynamics of Multifrequency coordination using parametric driving. J. Sport Exerc. Psych suppl. **23** (2001) 95
4. Batchelo,r P.G., Hill, D.L.G., Calamante, F., Atkinson, D.: Study of connectivity in the brain using the full diffusion tensor from MRI. in: Insana M.F., Leahy R.M. (eds.), Information Processing in Medical Imaging, 120-133, Springer Lecture Notes in Computer Science (2001)
5. Braitenberg, V., Schüz A.: Anatomy of the cortex. Statistics and geometry. Springer, Berlin (1991)
6. Borland, L., Haken, H.: Unbiased determination of forces causing observed processes. The case of additive and weak multiplicative noise. Z. Phys. B - Condensed Matter **81** (1992) 95
7. Borland, L.: Learning the dynamics of two-dimensional stochastic Markov processes. Open Sys. & Inf. Dyn. **1** (1992) 3
8. Conolly, K., Stratton, P.: Developmental changes in associated movements. Dev. Med. Child. Neurol. **10** (1968) 49–56
9. Dale, A., Fischl, B., Sereno, M.I.: Cortical Surface-Based Analysis I. Neuroimage **9** (1999) 179–194
10. Fischl, B., Sereno, M.I., Dale, A.: Cortical Surface-Based Analysis II. Neuroimage **9** (1999) 195–207
11. Felleman, D.J., Van Essen, D.C.: Distributed hierarchical processing in the primate cerebral cortex. Cerebral Cortex **1** (1991) 1–47
12. Fink, P., Foo, P., Jirsa, V.K., Kelso, J.A.S.: Local and global stabilization of coordination by sensory information. Exp. Brain Res. **134** (2000) 9–20
13. Frank, T.D., Daffertshofer, A., Peper, C.E., Beek, P.J., Haken, H.: Towards a comprehensive theory of barin activity: Coupled oscillator systems under external forces. Physica D **144** (2000) 62–86
14. Freeman, W.J.: Tutorial on neurobiology: From single neurons to brain chaos. Inter. Journ. Bif. Chaos **2** (1992) 451–482
15. Fuchs, A., Kelso, J.A.S., Haken, H.: Phase Transitions in the Human Brain: Spatial Mode Dynamics. Inter. Journ. Bif. Chaos **2** (1992) 917–939
16. Fuchs, A., Jirsa, V.K., Kelso, J.A.S.: Theory of the relation between human brain activity (MEG) and hand movements. Neuroimage **11** (2000) 359–369
17. Fuchs, A., Mayville, J.M., Cheyne, D., Weinberg, H., Deecke, L., Kelso, J.A.S.: Spatiotemporal analysis of neuromagnetic events underlying the emergence of coordinative instabilities. Neuroimage **12** (2000) 71–84

18. Haken, H.: Synergetics. An Introduction. 3rd ed., Springer, Berlin Heidelberg New York (1983)
19. Haken, H., Kelso, J.A.S., Bunz, H.: A Theoretical Model of Phase transitions in Human Hand Movements. Biol. Cybern. **51** (1985) 347–356
20. Haken, H.: Advanced Synergetics. 2nd ed., Springer, Berlin Heidelberg New York (1987)
21. Haken, H.: Principles of brain functioning. Springer, Berlin Heidelberg New York (1996)
22. Haken, H.: What can Synergetics contribute to the understanding of brain functioning? in: Uhl C. (ed.), Analysis of neurophysiological brain functioning, Springer Berlin (1999)
23. Hale, J., Kocak, H.: Dynamics and Bifurcations. Springer, New York Berlin Heidelberg (1996)
24. Hämäläinen, M., Sarvas, J.: Realistic conductivity geometry model of the human head for interpretation of neuromagnetic data. IEEE Trans. Biomed. Engin. **36** (1989) 3 165171
25. Hämäläinen, M., Hari, R., Ilmoniemi, R.J., Knuutila, J., Lounasmaa, O.V.: Magnetoencephalography - theory, instrumentation, and applications to noninvasive studies of the working human brain. Rev. Mod. Phys. **65** (1993) 2 413–497
26. Ivry, R.: Cerebellar timing systems. Cerebellum and Cognition. Intern. Rev. of Neurobio. **41** (1997) 555–573
27. Jäncke, L., Peters, M., Himmelbach, M., Nösselt, T., Shah, J., Steinmetz, H.: fMRI study of bimanual coordination. Neuropsychologia **38** (2000) 164–174
28. Jantzen, K.J., Fuchs, A., Mayville, J., Deecke, L., Kelso, J.A.S.: Alpha and beta band changes in MEG Reflect Learning Induced Increases in Coordinative Stability. submitted to Clin. Neurophys. (2000)
29. Jirsa, V.K., Friedrich, R., Haken, H., Kelso, J.A.S.: A theoretical model of phase transitions in the human brain. Biol. Cybern. **71** (1994) 27-35
30. Jirsa, V.K., Friedrich, R., Haken, H.: Reconstruction of the spatio-temporal dynamics of a human magnetoencephalogram. Physica D **89** (1995) 100–122
31. Jirsa, V.K., Haken, H.: Field theory of electromagnetic brain activity. Phys. Rev. Let. **77** (1996) 960–963
32. Jirsa, V.K., Haken, H.: A derivation of a macroscopic field theory of the brain from the quasi-microscopic neural dynamics. Physica D **99** (1997) 503–526
33. Jirsa, V.K., Fuchs, A., Kelso, J.A.S.: Connecting cortical and behavioral dynamics: bimanual coordination. Neur. Comp. **10** (1998) 2019–2045
34. Jirsa, V.K., Fink, P., Foo, P., Kelso, J.A.S.: Parametric stabilization of biological coordination: a theoretical model. J. Biol. Phys. **26** (2000) 85–112
35. Jirsa, V.K.: Dimension reduction in pattern forming systems with heterogeneous connection topologies. Prog. Theo. Phys. Suppl. **139** (2000) 128–138
36. Jirsa, V.K., Kelso, J.A.S.: Spatiotemporal pattern formation in neural systems with heterogeneous connection topologies. Phys. Rev. E **62** (2000) 8462–8465
37. Kelso, J.A.S.: On the oscillatory basis of movement. Bull. Psychon. Soc. **18** (1981) 63
38. Kelso, J.A.S., Bressler, S.L., Buchanan, S., DeGuzman, G.C., Ding, M., Fuchs, A., Holroyd, T.: A phase transition in human brain and behavior. Phys. Let. A **169** (1992) 134–144
39. Kelso, J.A.S.: Dynamic Patterns. The Self-Organization of Brain and Behavior. The MIT Press, Cambridge, Massachusetts (1995)

40. Kelso, J.A.S., Jirsa, V.K., Fuchs, A.: Traversing scales of organization in brain and behavior: Experiments and concepts. In: Uhl, C. (ed.), Analysis of neurophysiological brain functioning, Springer Berlin (1999) 73–125
41. Kelso, J.A.S., Fuchs, A., Lancaster, R., Holroyd, T., Cheyne, D., Weinberg, H.: Dynamic cortical activity in the human brain reveals motor equivalence. Nature **23** (1998) 814–818
42. Knuth, K.: A Bayesian approach to source separation. in: Cardoso, J.F., Jutten, C., Loubaton, P. (eds.), Proceedings of the First International Workshop on Independent Component Analysis and Signal Separation (1999) 283–288
43. Kuramoto, Y.: Chemical oscillations, waves, and turbulence. Springer Berlin Heidelberg New York Tokyo(1984)
44. Kwapien, J., Drozdz, S., Liu, L.C., Ioannides, A.A.: Cooperative dynamics in auditory brain response. Phys. Rev. E **58** (1998) 6359–6367
45. Kwasniok, F.: The reduction of complex dynamical systems usig principal interaction patterns. Physica D **92** (1996) 28–60
46. Kwasniok, F.: Optimal Galerkin approximations of partial differential equations using principal interaction patterns. Phys. Rev. E **55** (1997) 5365–5375
47. Liley, D.T.J., Cadusch, P.J., Wright, J.J.: A continuum theory of electrocortical activity. Neurocomputing **26-27** (1999) 795
48. Makeig, S., Bell, A.J., Jung, T.P., Sejnowski, T.J.: Independent component analysis of electroencephalic data. in: Touretsky, D., Mozer, M., Hasselmo, M. (eds.), Advances in neural information processing systems. Vol. 8 145–151 MIT Press, Cambridge (1996)
49. Mayville, J.M., Bresssler, S.L., Fuchs, A., Kelso, J.A.S.: Spatiotemporal reorganization of electrical activity in the human brain asscoiated with timing transition in rhythmic auditory-motor coordination. Exp. Brain Res. **127** (1999) 371–381
50. Meyer, U.M., Röricht, S., von Einsiedel, H., Kruggel, F., Weindl, A.: Inhibitory and excitatory interhemispheric transfers between motor cortical areas in normal humans and patients with abnormalities of corpus callosum. Brain **118** (1995) 429–440
51. Mosher, J.C., Baillet, S., Leahy, R.M.: EEG source localization and imaging using multiple signal classification approaches. J. Clin. Neurophys. **16** (1999) 225–238
52. Nunez, P.L.: The brain wave equation: A model for the EEG. Mathematical Biosciences **21** (1974) 279–297
53. Nunez, P.L.: Neocortical dynamics and human EEG rhythms. Oxford University Press (1995)
54. Parker, G.J.M., Wheeler-Kingshott, C.A.M., Barker, G.J.: Distributed anatomical brain connectivity derived from diffusion tensor inaging. in: Insana M.F., Leahy R.M. (eds.), Information Processing in Medical Imaging, 106-120, Springer Lecture Notes in Computer Science (2001)
55. Robinson, P.A., Rennie, C.J., Wright, J.J.: Propagation and stability of waves of electrical activity in the cerebral cortex. Phys. Rev. E **56** (1997) 826
56. Sadato, N., Yonekura, Y., Waki, A., Yamada, A., Ishii, Y.: Role of the supplementary motor area and the right premotor cortex in the coordination of bimanual finger movements. Journ. Neurosc. **17** (24), (1997) 9667-9674
57. Sclar, G., Maunsell, J.H.R., Lennie, P.: Coding of image contrast in central visual pathways of the macaque monkey. Vision Res. **30** (1990) 1-10
58. Steyn-Ross, M.L., Steyn-Ross, D.A., Sleigh, J.W., Liley, D.T.J.: Theoretical EEG stationary spectrum for a white-noise-driven cortex. Phys. Rev. E **60** (1999) 7299
59. Uhl, C., Friedrich, R., Haken, H.: Analysis of spatio-temporal signals of complex systems. Phys Rev. E **51** (1995) 3890–3900

60. Uhl, C. (ed.): Analysis of neurophysiological brain functioning, Springer Berlin (1999)
61. Williamson, S.J., Kaufman, L.: Analysis of neuromagnetic signals. in: Gevins A.S., Remond A. (eds.), Methods of analysis of brain electrical and magnetic signals. EEG Handbook, Elsevier Science (1987)
62. Wilson, H.R., Cowan, J.D.: Excitatory and inhibitory interactions in localized populations of model neurons. Biophysical Journal **12** (1972) 1–24
63. Wilson, H.R., Cowan, J.D.: A mathematical theory of the functional dynamics of cortical and thalamic nervous tissue. Kybernetik **13** (1973) 55–80
64. Wright, J.J., Liley, D.T.J.: Dynamics of the brain at global and microscopic scales: Neural networks and the EEG. Behav. Brain. Sci. **19** (1996) 285
65. Yakovlev, P.I., Lecours, A.R.: The myelogenetic cycles of regional maturation of the brain. in: Minkowski A. (ed.) Development of the brain in early life. Blackwell, Oxford (1967) 3-70